

# Phase Ordering and Onset of Collective Behavior in Chaotic Coupled Map Lattices

Anaël Lemaître<sup>(1,2)</sup> and Hugues Chaté<sup>(2,1)</sup>

<sup>(1)</sup>*LadHyX, Laboratoire d'Hydrodynamique, Ecole Polytechnique, 91128 Palaiseau, France*

<sup>(2)</sup>*CEA, Service de Physique de l'Etat Condensé, Centre d'Etudes de Saclay, 91191 Gif-sur-Yvette, France*  
(April 26, 2024)

The phase ordering properties of lattices of band-chaotic maps coupled diffusively with some coupling strength  $g$  are studied in order to determine the limit value  $g_e$  beyond which multistability disappears and non-trivial collective behavior is observed. The persistence of equivalent discrete spin variables and the characteristic length of the patterns observed scale algebraically with time during phase ordering. The associated exponents vary continuously with  $g$  but remain proportional to each other, with a ratio close to that of the time-dependent Ginzburg-Landau equation. The corresponding individual values seem to be recovered in the space-continuous limit.

One of the most remarkable features distinguishing extensively-chaotic dynamical systems from most models studied in out-of-equilibrium statistical physics is that they generically exhibit non-trivial collective behavior (NTCB), i.e. long-range order emerging out of local chaos, accompanied by the temporal evolution of spatially-averaged quantities [1–3]. In particular, NTCB is easily observed on simple models of reaction-diffusion systems such as coupled map lattices (CMLs) in which (chaotic) nonlinear maps  $S$  of real variables  $X$  are coupled diffusively with some coupling strength  $g$  [3].

NTCB is often claimed to be a *macroscopic* attractor, well-defined in the infinite-size limit and reached for almost every initial condition, provided the local coupling between sites is “large enough”. On the other hand, for small  $g$  values, such as those corresponding to the so-called “anti-integrable” limit which tries to extend zero-coupling behavior to small, but finite coupling strengths, CMLs often exhibit multistability [4]. This is in particular the case if the local map shows banded chaos, because the interfaces separating clusters of sites in the different bands can be pinned. This multistability is “extensive”: the number of (chaotic) attractors may then be argued to grow exponentially with the system size, in opposition to NTCB for which this number is small and size-independent.

In this Letter, we define and measure the limit coupling strength  $g_e$  separating the strong-coupling regime in which NTCB is observed from the weak-coupling, extensive multistability region. Using the discrete “spin” variables which can be defined whenever the one-body probability distribution functions (pdfs) of local (continuous) variables have disjoint supports, we study numerically the phase ordering process following uncorrelated initial conditions in cases where the spin variables take only two values. We find that the persistence probability  $p(t)$  (i.e. the proportion of spins which have not changed sign up to time  $t$ ) saturates in finite time to strictly positive values in the weak coupling regime whereas it de-

cays algebraically to zero when  $g > g_e$ . The associated persistence exponent  $\theta$  varies continuously with parameters, at odds with traditional models [5]. Moreover, data obtained on various two-dimensional CMLs is best accounted for by a relation of the form  $\theta \sim (g - g_e)^w$ , which we use to estimate  $g_e$ . We show further that this behavior is mostly due to the non-trivial scaling of the characteristic length  $L(t) \sim t^\phi$  during the phase ordering process. Indeed,  $\phi \neq \frac{1}{2}$ , the expected value for a scalar, non-conserved order parameter [7], and is found to be proportional to  $\theta$ , with the exponent ratio  $\phi/\theta$  approximately taking the value known for the time-dependent Ginzburg-Landau equation (TDGLE). We also provide evidence that, in the continuous-space limit, “normal” phase ordering behavior is recovered. Finally, we discuss the hierarchy of limit coupling values  $g_e^n$  which can be defined when the local map is unimodal and shows  $2^n$ -band chaos, using recent results on renormalisation group (RG) ideas applied to CMLs [8].

Consider a  $d$ -dimensional hypercubic lattices  $\mathcal{L}$  of coupled identical maps  $S_\mu$  acting on real variables  $(X_{\vec{r}})_{\vec{r} \in \mathcal{L}}$ :

$$X_{\vec{r}}^{t+1} = (1 - 2dg)S_\mu(X_{\vec{r}}^t) + g \sum_{\vec{e} \in \mathcal{V}} S_\mu(X_{\vec{r}+\vec{e}}^t), \quad (1)$$

where  $\mathcal{V}$  is the set of  $2d$  nearest neighbors  $\vec{e}$  of site  $\vec{0}$ . We first present results obtained for the piecewise linear, odd, local map  $S_\mu$  defined by:

$$S_\mu(X) = \begin{cases} \mu X & \text{if } X \in [-1/3, 1/3] \\ 2\mu/3 - \mu X & \text{if } X \in [1/3, 1] \\ -2\mu/3 - \mu X & \text{if } X \in [-1, -1/3] \end{cases} \quad (2)$$

which leaves the  $I = [-1, 1]$  interval invariant. (For  $\mu = 3$ , this is the chaotic map introduced by Miller and Huse [9].) For  $\mu \in [-2, -1]$ ,  $S_\mu$  displays banded chaos, while for opposite  $\mu$  values, these bands become invariant subintervals of  $I$ . At  $\mu = 1.9$  in particular,  $S_\mu$  possesses two symmetric such intervals  $I^\pm = [\pm\mu(2 - \mu)/3, \pm\mu/3]$ , separated by a finite gap. For any value of  $g$ , the support of the pdf of  $X$  for the CML defined by (1-2) can be

separated into two components thanks to the symmetry of the map. This allows the unambiguous definition of spin variables  $\sigma_{\vec{r}} = \text{sign}(X_{\vec{r}})$ . The deterministic nature of the system and the form of the coupling strictly forbids the nucleation of opposite-phase droplets in clusters: the analog spin system is at zero temperature.

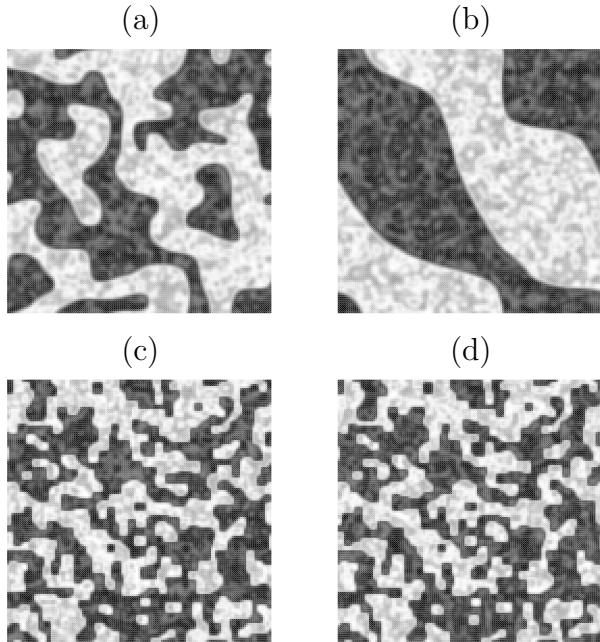


FIG. 1. Snapshots of the  $d = 2$  CML with local map (2). Lattice of  $128^2$  sites, grey scale from  $X = -1$  (white) to  $X = 1$  (black), uncorrelated initial conditions. (a,b): transient leading to complete ordering at  $g = 0.2 > g_e$ ,  $t = 100$  and  $1000$ ; (c,d): blocked state at  $g = 0.15 < g_e$ ,  $t = 1000$  and  $2000$ .

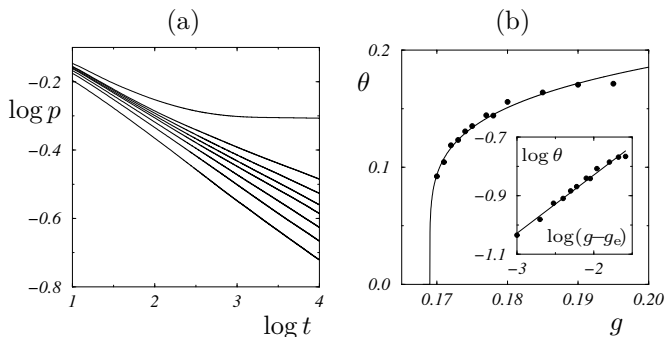


FIG. 2. Phase ordering in the  $d = 2$  CML with local map (2) at  $\mu = 1.9$ . (a): algebraic decay of the persistence probability  $p(t)$  for, from top to bottom:  $g = 0.16 (< g_e)$ : saturates to a finite level),  $0.17, 0.172, 0.174, 0.176, 0.18, 0.185$ , and  $0.195$ . (b): variation of persistence exponent  $\theta$  with  $g$ . Solid line: fitting Ansatz  $\theta \sim (g - g_e)^w$  with  $g_e = 0.169(1)$  and  $w = 0.20(3)$  Insert:  $\log(\theta)$  vs.  $\log(g - g_e)$ .

For large  $g$  values, complete phase ordering occurs (Fig. 1a,b), and the system eventually reaches a regime in which all sites are situated in one of the two intervals  $I^\pm$ . For small  $g$ , initial conditions with sites in both intervals  $I^\pm$  lead to spatially-blocked configurations where inter-

faces between clusters of each phase are strictly pinned, while chaos is present within clusters (Fig. 1c,d). [10]

To study the phase ordering process efficiently, uncorrelated initial conditions were generated as follows: exactly one half of the sites of a  $d = 2$  lattice were chosen at random and assigned positive  $X$  values drawn according to the invariant distribution of  $S_\mu$  on  $I^+$ , while the other sites were similarly assigned negative values. Large lattices with periodic boundary conditions were used, and the persistence  $p(t)$  was measured. Fig. 2a shows the results of single runs for various values of  $g$ . For small  $g$ ,  $p(t)$  saturates at large times to strictly positive values, while it decays algebraically, for large  $g$ , on square lattices of linear size 2048 sites. The associated persistence exponent  $\theta$  varies continuously with  $g$ , and its  $g$ -dependence is nicely accounted for by a functional form  $\theta \sim (g - g_e)^w$  with  $g_e \simeq 0.169(1)$  and  $w \simeq 0.20(3)$  (Fig. 2b). We have, at this point, no theoretical justification of this fitting Ansatz. At any rate, it provides an operational definition of  $g_e$  yielding estimates consistent with those obtained using other, less accurate, methods [11].

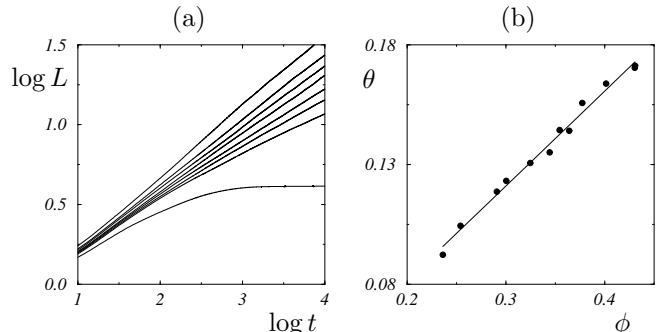


FIG. 3. Same runs as in Fig. 2. (a)  $\log(L)$  vs  $\log(t)$  (bottom curve:  $g = 0.16$ , top curve  $g = 0.195$ ); (b)  $\theta(g)$  vs  $\phi(g)$  for  $g$  values between  $0.17$  and  $0.20$ ; the solid line is the linear fit  $\theta \simeq 0.396\phi - 0.002$ .

The origin of this unusual behavior of the persistence exponent is largely explained by the evolution of the spatial structures formed during phase ordering. Usually, one expects the coarsening to be described by the algebraic growth of a single characteristic length  $L(t) \sim t^\phi$  with  $\phi = 1/2$  for a non-conserved, scalar order parameter [7]. In the CML studied above, the two-point correlation function  $C(\vec{x}, t) = \langle \sigma_{\vec{r}+\vec{x}}^t \sigma_{\vec{r}}^t \rangle$  was measured during phase ordering [12]. Length  $L(t)$  was then evaluated to be the width at mid-height ( $C(L(t), t) = 1/2$ ), determined by interpolation. This procedure was then validated by a collapse of all  $C(\|\vec{x}\|/L(t), t)$  curves. Surprisingly, while the scaling behavior of  $L(t)$  is observed, exponent  $\phi$  departs from the expected  $1/2$  value and varies continuously with  $g$  (Fig. 3). Again, we find a law of the form  $\phi \sim (g - g_e)^w$  to be an acceptable Ansatz of our numerical results. The estimated values of  $g_e$  and  $w$  are consistent, within numerical accuracy, with those found when fitting  $\theta(g)$ . This is corroborated by studying directly  $p(t)$  vs

$L(t)$  (not shown), or by plotting  $\theta$  vs  $\phi$  which confirms that the two exponents are proportional to each other (Fig. 3d). Remarkably, the ratio  $\theta/\phi$  is found to have, within our numerical accuracy, the  $d = 2$  TDGLE value:  $\theta/\phi \simeq 0.40(2) \simeq 2\theta_{\text{GL}} \simeq 0.40$  [13]. (We cannot, however, completely exclude the values corresponding to the Ising model, or the diffusion equation, since  $\theta_{\text{Ising}} \simeq 0.22$  [14], and  $\theta_{\text{Diff.}} \simeq 0.19$  [13].)

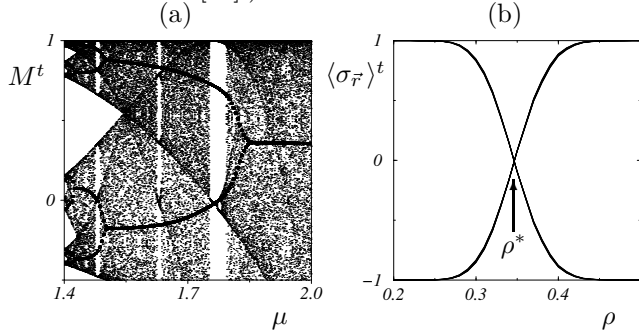


FIG. 4.  $d = 2$  lattice of coupled logistic maps for  $g = 0.2$ . (a) bifurcation diagram ( $\langle X_{\bar{r}}^t \rangle$ , large dots) superimposed on that of single logistic map (small dots). (b):  $\langle \sigma_{\bar{r}}^t \rangle$  vs  $\rho$  plotted at 20 different timesteps between  $t = 500$  and  $t = 1000$  for  $\mu_2^c < \mu = 1.5 < \bar{\mu}_2$ . This “magnetization” remains constant only for  $\rho = \rho^* \simeq 0.3465$ , whereas it reflects the overall period-2 dynamics for all other  $\rho$  values. (c)  $\theta(g)$  at  $\mu = 1.5$  and  $\rho = \rho^*(g)$  with log-log fit ( $g_e \simeq 0.101$ ,  $w \simeq 0.06$ ). (d)  $\theta(g)$  vs  $\phi(g)$ ; the solid line is the linear fit  $\theta \simeq 0.40\phi - 0.002$ .

The same analysis was also performed on CMLs with a non-symmetric, unimodal, local map  $S_\mu$  of the form:

$$S_\mu(X) = 1 - \mu|X|^{1+\varepsilon} \quad \text{with } \mu \in [0, 2], \quad (3)$$

in particular for  $\varepsilon = 0$  (tent map) and  $\varepsilon = 1$  (logistic map). For  $\mu \in [\mu_\infty, 2]$ , this map shows  $2^n$ -band chaos and exhibits an inverse cascade of band-merging points  $\bar{\mu}_n$  when  $\mu \rightarrow \mu_\infty$ . In the strong-coupling limit, the corresponding CMLs exhibit, depending on  $d$ , periodic or quasiperiodic NTCB with a period equal to, or a multiple of, that of the band-chaos of the local map [3,8]. For  $d = 2$  and 3, in particular, simple period- $2^n$  NTCB occurs, with an infinite cascade of phase transition points  $\mu_n^c$  distinct from the band-merging points (Fig. 4a). When period-2 NTCB occurs in the two-band chaotic region of the map ( $\mu \in [\bar{\mu}_2, \bar{\mu}_1] \approx [1.43, 1.54]$ ), two-state spin variables  $\sigma_{\bar{r}}^t \in \{-1, 1\}$  can be defined, but the asymmetry of the two bands hinders the generation of “effectively” uncorrelated initial conditions. Indeed, an equal proportion of sites in each band quickly leads to complete phase ordering and saturation of  $p(t)$ , even in the strong-coupling regime. This happens because these initial conditions create, after a few timesteps, configurations with a fairly large unbalance between the two phases. Tuning the initial proportion  $\rho$  of sites in, say, the band containing  $X = 0$ , one can minimize such effects. We determined the optimal proportion  $\rho^*$  defined as the value for which the magnetization  $\langle \sigma_{\bar{r}}^t \rangle$  remains

constant (Fig. 4b). Clean scaling behavior of  $L(t)$  and  $p(t)$  is then observed with reasonable system sizes, as with the symmetric local map (2). Varying the coupling strength  $g$ , exponents  $\phi$  and  $\theta$  show the same behavior as above, decreasing continuously to zero at  $g_e$ . Fig. 4c shows the case of coupled logistic maps, for which the Ansatz  $\theta, \phi \sim (g - g_e)^w$  is, again, valid, although not as good as in the case of local map (2). Note that the estimated value  $w \simeq 0.06(2)$  is different from that measured for the CML with local map (2), but  $\theta/\phi \simeq 0.48(4)$  is still rather close to the TDGLE value (Fig. 4d).

We now deal with the onset of more complex NTCB such as the period- $2^n$  cycles mentioned above for which the study of the phase ordering in terms of two-state spin variables may not be legitimate.

Consider, for example, a CML with local map  $S_\mu$  defined by (3) in a 4-band chaotic regime ( $\mu \in [\bar{\mu}_3, \bar{\mu}_2]$ ) which exhibits period-4 NTCB. The “natural” spin variables to study phase ordering take four values, indexed by the 4-band chaotic cycle. However, these four bands can be grouped in two “meta-bands”, since they arise from a band splitting bifurcation at  $\bar{\mu}_2$ , so that two-state spin variables can still be defined. Accordingly, two limit coupling strengths can be defined:  $g_e^1$ , marking the onset of complete phase ordering between the two meta-bands, and  $g_e^2$  for ordering from initial conditions within one of the meta-bands. A priori,  $g_e^2 \neq g_e^1$ , and there might exist coupling strengths such that, e.g., pinned clusters exist within, but not between, the two meta-bands. The “true” onset of period-4 NTCB is then given by  $g \geq \max(g_e^1, g_e^2)$ . Similarly, for  $\mu \in [\mu_\infty, \bar{\mu}_n]$ , one can define  $n$  different  $\mu$ -dependent limit coupling strengths  $g_e^1, g_e^2, \dots, g_e^n$ , with  $n \rightarrow \infty$  as  $\mu \rightarrow \mu_\infty$ . Using our recent work on renormalisation group arguments for CMLs [8], one can show that the threshold values of this infinite hierarchy are related to each other. Here, we only describe briefly these results, while a detailed derivation can be found in [8]. The RG structure of single map (3) induces the conjugacy between  $(\Delta_g^m \circ \mathbf{S}_\mu)^2$  and  $\Delta_g^{2m} \circ \mathbf{S}_{q(\mu)}$ , where  $\mathbf{S}_\mu$  transforms each variable  $X_{\bar{r}}$  by  $S_\mu$ ,  $\Delta_g^m$  is the diffusive operator applied  $m$  times, and  $q(\mu) = \mu^2$  for coupled tent maps. This relation can be shown to imply that  $g_e^2(\mu, m) = g_e^1(q(\mu), 2m)$ . Furthermore, using the fact that  $g_e^n(\mu, m)$  decreases with  $m$ , one can prove that the maximum  $g_e$  for all  $n, \mu$ , and  $m$  is  $g_e^* = g_e^1(\bar{\mu}_1, 1)$ . Thus, whenever  $g \geq g_e^*$ , complete ordering occurs for all bands.

The above results are at odds with the behavior of usual models studied in phase ordering problems [15]. But in both cases presented here, the exponent ratio  $\theta/\phi$  seems to take the value expected for the TDGLE model. This “weak universality” is reminiscent of similar results found recently at the Ising-like critical points shown by the same models [16]. We note, moreover, that, when  $g$  is increased,  $\phi$  approaches  $1/2$  and  $\theta$  reaches values close to  $\theta_{\text{GL}}$ . We believe that this tendency is mostly due to

the lattice effects becoming less and less important (although strict pinning does not occur for  $g > g_e$ ). We have shown recently [8] that, in the continuous-space limit of CMLs, the weak coupling regime disappears ( $g_e \rightarrow 0$ ), together with any pinning effects. One can thus wonder whether, in this limit, one recovers more “conventional” phase ordering dynamics.

The continuous limit of CMLs such as those defined by (1-2) is reached when applying the coupling step of the dynamics more and more times per iteration, i.e. when taking the  $m \rightarrow \infty$  limit of  $\Delta_g^m \circ \mathbf{S}_\mu$ . In this limit,  $\Delta_g^m$  converges to a universal Gaussian kernel  $\Delta_\lambda^\infty = \exp(\frac{\lambda^2}{2}\nabla^2)$  with a coupling range  $\lambda = \sqrt{2gm}\|\vec{e}\|$  where  $\|\vec{e}\|$  is the lattice spacing, which can thus be chosen to scale like  $1/\sqrt{m}$  so as to keep  $\lambda$  constant. We investigated the phase ordering properties of these CMLs with the symmetric local map (2) for increasing values of  $m$ . At a qualitative level, the scaling behavior of  $L(t)$  and  $p(t)$  is observed at all  $m$  values. Quantitatively, exponents  $\theta$  and  $\phi$  vary with  $m$  at fixed  $g$ . Increasing  $m$ ,  $\phi$  seems to converge to 1/2, while  $\theta \rightarrow \theta_{GL}$ : for  $m = 1$  to 3, we find  $\phi = 0.467, 0.479, 0.505$ , and  $\theta = 0.174, 0.184, 0.196$ , from single runs on lattices of linear size 4096 sites.

Our work provides a quantitative method for determining the onset of NTCB in chaotic coupled map lattices. It also reveals that the phase-ordering properties of multiphase, chaotic CMLs are different from those of most models studied traditionally. More work is needed, especially at the analytical level, to clarify the origin of the non-universality observed and put our numerical results on firmer ground, since we cannot completely exclude a very slow, unobservable, crossover of the scaling behavior observed to that of a more traditional model. Different approaches can be suggested.

A continuous variation of the scaling exponent  $\phi$  for the characteristic length of domains is not usually observed, but (at least) two exceptions are known. One is the case of coarsening from initial conditions with built-in long-range correlations [17], but then the persistence probability  $p(t)$  does *not* decrease algebraically with time [18]. Another situation of possible relevance is the case of phase-ordering with an order-parameter-dependent mobility [19], for which, unfortunately, the behavior of the persistence is not known. At any rate, the recovery of the “normal” scaling properties of the TDGLE in the space-continuous limit suggests that lattice effects are ultimately responsible for the non-trivial scaling properties recorded in discrete systems. This calls for a detailed study of interface dynamics in order to assess the effective

role of discretization and anisotropy.

Finally, we believe our results are general and that similar behavior should be found in experiments on phase-ordering of pattern-forming systems, such as, e.g., electro-hydrodynamical convection in liquid crystals, or Rayleigh-Bénard convection [20].

We thank Ivan Dornic for many fruitful discussions and his keen interest in our work.

- 
- [1] H. Chaté, Int. J. Mod. Phys. B **12**, 299 (1998).
  - [2] J. A. C. Gallas et al., Physica A **180**, 19 (1992); J. Hemmingsson, Physica A **183**, 255 (1992); H. Chaté and P. Manneville, Europhys. Lett. **14**, 409 (1991); H. Chaté, L.-H. Tang, and G. Grinstein, Phys. Rev. Lett. **74**, 912 (1995).
  - [3] H. Chaté and P. Manneville, Prog. Theor. Phys. **87**, 1 (1992); Europhys. Lett. **17**, 291 (1992); H. Chaté and J. Losson, Physica D **103**, 51 (1997).
  - [4] R.S. MacKay and T.A. Sépulchre, Physica D **82**, 243 (1995); T.A. Sépulchre and R.S. MacKay, Nonlinearity **10**, 679 (1997); S. Aubry, Physica D **103**, 201 (1997).
  - [5] See, e.g.: I. Dornic and C. Godrèche, J. Phys. A **31**, 5413 (1998), and references therein.
  - [6] D. Stauffer, J. Phys. A **27**, 5029 (1994).
  - [7] P.C. Hohenberg and B.I. Halperin, Rev. Mod. Phys. **49**, 436 (1977).
  - [8] A. Lemaître and H. Chaté, Phys. Rev. Lett. **80**, 5528 (1998); preprint, 1998.
  - [9] J. Miller and D.A. Huse, Phys. Rev. E **48**, 2528 (1993).
  - [10] In CMLs, pinning can be strict (the “effective noise” arising from local chaos is bounded). It is *local*, and thus no finite-size effect is observed for large-enough systems.
  - [11] A. Lemaître, Ph.D. thesis, Ecole Polytechnique, 1998.
  - [12] The same analysis was also performed using the continuous variables  $X_{\vec{r}}$ , yielding similar, albeit noisier, results.
  - [13] S. Cueille and C. Sire, “Block persistence”, cond-mat/9803014; S. H. Cornell, private communication.
  - [14] D. Stauffer, J. Phys. A **27**, 5029 (1994).
  - [15] A.J. Bray, Adv. Phys. **43**, 357 (1994).
  - [16] P. Marcq, H. Chaté, and P. Manneville, Phys. Rev. Lett. **77**, 4003 (1996); Phys. Rev. E **55**, 2488 (1997).
  - [17] B. Derrida, C. Godrèche, and I. Yekutieli, Phys. Rev. A **44**, 6241 (1991).
  - [18] H. Nakanishi, H. Chaté, and I. Dornic, unpublished.
  - [19] C.L. Emmott and A.J. Bray, preprint cond-mat/9808308.
  - [20] M.C. Cross and D.I. Meiron, Phys. Rev. Lett. **75**, 2152 (1995).